

AdaBrowse: Adaptive Video Browser for Efficient Continuous Sign Language Recognition

Lianyu Hu
Tianjin University, China
hly2021@tju.edu.cn

Liqing Gao
Tianjin University, China
lqgao@tju.edu.cn

Zekang Liu
Tianjin University, China
lzk100953@tju.edu.cn

Chi-Man Pun
University of Macau, China
cmpun@umac.mo

Wei Feng
Tianjin University, China
wfeng@ieee.org

ABSTRACT

Raw videos have been proven to own considerable feature redundancy where in many cases only a portion of frames can already meet the requirements for accurate recognition. In this paper, we are interested in whether such redundancy can be effectively leveraged to facilitate efficient inference in continuous sign language recognition (CSLR). We propose a novel adaptive model (AdaBrowse) to dynamically select a most informative subsequence from input video sequences by modelling this problem as a sequential decision task. In specific, we first utilize a lightweight network to quickly scan input videos to extract coarse features. Then these features are fed into a policy network to intelligently select a subsequence to process. The corresponding subsequence is finally inferred by a normal CSLR model for sentence prediction. As only a portion of frames are processed in this procedure, the total computations can be considerably saved. Besides temporal redundancy, we are also interested in whether the inherent spatial redundancy can be seamlessly integrated together to achieve further efficiency, i.e., dynamically selecting a lowest input resolution for each sample, whose model is referred to as AdaBrowse+. Extensive experimental results on four large-scale CSLR datasets, i.e., PHOENIX14, PHOENIX14-T, CSL-Daily and CSL, demonstrate the effectiveness of AdaBrowse and AdaBrowse+ by achieving comparable accuracy with state-of-the-art methods with 1.44× throughput and 2.12× fewer FLOPs. Comparisons with other commonly-used 2D CNNs and adaptive efficient methods verify the effectiveness of AdaBrowse. Code is available at <https://github.com/hulianyuuy/AdaBrowse>.

CCS CONCEPTS

• **Computing methodologies** → **Activity recognition and understanding; Supervised learning; Neural networks.**

KEYWORDS

Continuous sign language recognition, efficient inference, feature redundancy.

Permission to make digital or hard copies of all or part of this work for personal or classroom use is granted without fee provided that copies are not made or distributed for profit or commercial advantage and that copies bear this notice and the full citation on the first page. Copyrights for components of this work owned by others than the author(s) must be honored. Abstracting with credit is permitted. To copy otherwise, or republish, to post on servers or to redistribute to lists, requires prior specific permission and/or a fee. Request permissions from permissions@acm.org.

MM '23, October 29–November 3, 2023, Ottawa, ON, Canada

© 2023 Copyright held by the owner/author(s). Publication rights licensed to ACM.

ACM ISBN 979-8-4007-0108-5/23/10...\$15.00

<https://doi.org/10.1145/3581783.3611745>

ACM Reference Format:

Lianyu Hu, Liqing Gao, Zekang Liu, Chi-Man Pun, and Wei Feng. 2023. AdaBrowse: Adaptive Video Browser for Efficient Continuous Sign Language Recognition. In *Proceedings of the 31st ACM International Conference on Multimedia (MM '23)*, October 29–November 3, 2023, Ottawa, ON, Canada. ACM, New York, NY, USA, 10 pages. <https://doi.org/10.1145/3581783.3611745>

1 INTRODUCTION

Sign language is one of the most important communication tools for the deaf people in their daily life. However, mastering this language is rather difficult and exhaustive for the hearing people, which severely hinders direct communication between the two groups. Continuous sign language recognition (CSLR) aims to automatically translate input sign videos into sentences, which may greatly relieve this dilemma and provide more non-intrusive communication channels for both groups. Despite great progress achieved by recent methods [3, 7, 29, 34, 35, 35–37, 50] upon accuracy in CSLR, they typically bring plenty of computations and cause a low throughput, which is especially undesirable towards real-life scenarios with demands of low computations and real-time processing.

In this paper, we aim to address this issue by leveraging the inherent feature redundancy in raw videos to save unnecessary computations, based on the observation that not all frames are equally important for CSLR. On the one hand, the shot video is usually information-intensive. One gloss¹ in a sign video always consumes tens of frames to record. However, our human beings could scan just few frames to recognize a sign, which shows that the involved information in videos is inherently redundant. Serially processing all frames may waste a lot of computations. On the other hand, we notice that different videos may require information of different degrees for recognition. For example, some sign videos are expressed with large body movements with few disturbances, which could be recognized with low resolutions easily. In contrast, the signs of some videos are quite similar which require detailed spatial features of high resolutions to recognize. The required computations are thus unevenly distributed across different videos. Thus, equally treating all videos with full images (224×224) may be unnecessary.

In this paper, we present AdaBrowse to leverage spatial and temporal feature redundancy to achieve efficient CSLR. For the temporal domain, we propose to dynamically select a subsequence of input videos to process to save unnecessary computations. As

¹Gloss is the atomic lexical unit to annotate sign languages.

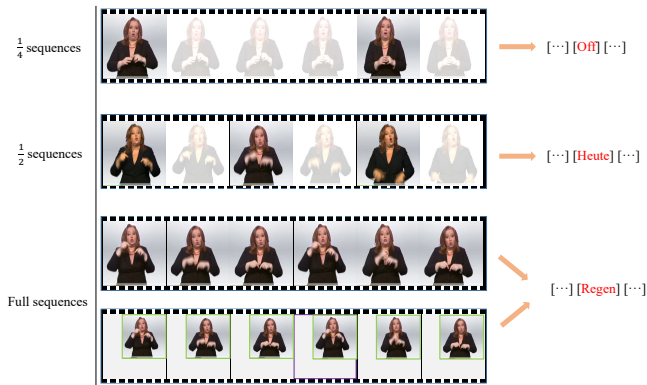


Figure 1: Videos in many cases can be accurately recognized from only a portion of frames or from small inputs (bottom).

shown in fig. 1, in our experiments we found "easy" videos of relatively small human movements and sparse spatial details, usually require fewer frames (e.g., $\frac{1}{4}$ and $\frac{1}{2}$). In contrast, "hard" videos always require an intact input sequence to fully explore frame correlations to reduce mistakes as much as possible. In specific, our model first utilizes a lightweight global convolutional neural network (CNN) to take a quick glance at input videos to extract cheap and coarse features. Then a recurrent policy network is trained based on these preceding features to select a most informative subsequence under limited computational costs. This procedure refers to the Gumbel-Softmax Algorithm [24] to tackle the non-differentiable problem resulting from discrete sampling from multiple subsequence candidates. Finally, we feed the corresponding subsequence into an attached CSLR model to perform sentence prediction. As only a portion of frames are processed in this procedure, the total computations can be considerably saved. For the spatial domain, we propose to adaptively switch the input resolution for each video to reduce unnecessary computations. This is based on the observation that many videos can be perfectly recognized in sequences of relatively small images (the bottom of fig. 1). This is achieved by naturally extending the policy network in AdaBrowse into a unified form to both determine input resolution and select a subsequence for processing, whose model is referred to as AdaBrowse+. As we show in the experiments, AdaBrowse series can intelligently learn to unevenly allocate computing resources among multiple subsequence candidates to balance between accuracy and computations.

Experimental results on four widely-used large-scale datasets, i.e., PHOENIX14, PHOENIX14-T, CSL-Daily and CSL, demonstrate AdaBrowse by itself can reduce a number of FLOPs² and achieve better throughput. AdaBrowse+ further promotes the efficiency to 2.12× fewer FLOPs and 1.44× better throughput. Comparisons with other commonly-used 2D CNNs and adaptive efficient methods verify the effectiveness of AdaBrowse. Notably, AdaBrowse series could achieve comparable accuracy with other heavy state-of-the-art methods, with much lower computations. Various in-depth analyses and visualizations are given to comprehensively show their effects from various perspectives.

²FLOPs denotes the number of multiply-add operations and GFLOPs denotes measuring FLOPs by giga.

2 RELATED WORK

2.1 Continuous Sign Language Recognition

Sign Language Recognition methods can be roughly categorized into isolated Sign Language Recognition (ISLR) and Continuous Sign Language Recognition (CSLR), and we focus on the latter one in this paper. Different from ISLR classifying a video into a single label, CSLR is a sequence-to-sequence task by translating input videos into target sentences, which is a potentially valuable tool for automatic sign video translation in real-life scenarios. Earlier methods [11, 13, 16, 26] in CSLR usually rely on hand-crafted features or Hidden Markov Model-based systems [27–29] to split videos and then perform translation. The recent success of CNNs and RNNs brings great progress for CSLR. Equipped with CTC loss [15] to align target sentences with predicted sentences for supervision, they [3, 5, 6, 6, 7, 34, 37] usually first employ a 2D CNN to extract frame-wise features, and then deploy hybrids of 1D CNNs and LSTM to capture temporal dependencies, followed by a classifier to perform sentence prediction. However, some methods [6, 7, 37] find that the 2D CNN is not well-trained in such a paradigm and propose to reuse the iterative training strategy to refine it, causing much longer training time and bringing more computations. More recent studies attempt to relieve this problem by directly enhancing the 2D CNN with extra modules and visual losses and [3, 17, 34] or squeezing beneficial temporal information [20]. Our method is orthogonal to and can be flexibly deployed upon these methods for efficient inference with preserved accuracy.

2.2 Reducing Temporal Redundancy

The inherent temporal redundancy in videos has been widely explored in related tasks based on the observation that not all frames contribute equally for recognition. Thus, a number of computations can be saved by paying less/no attention to less informative frames. These related methods can be roughly divided as follows: (1) early stopping [9, 14], where these methods propose to adaptively terminate the computation once a target prediction confidence threshold is met to save the following computations; (2) frame sampling [12, 30, 40, 42, 43], i.e., dynamically selecting a portion of input frames to process and discarding the rest; (3) conditional computing [32, 44], e.g., conditionally extracting coarse or expensive features at each timestep through a decision-maker to save unnecessary computations over less important frames. Besides the above-mentioned methods, Adafuse [33] proposes to dynamically decide whether to reuse features from past timesteps to save computations. Our AdaBrowse differentiates from these methods in a novel way to reduce temporal redundancy by selecting one optimal subsequence to process, with an implicit assumption that there is always a shortest subsequence containing most necessary information for recognition in each video.

2.3 Reducing Spatial Redundancy

Spatial redundancy has been broadly visited by previous methods in 2D image domain to reduce computations. Based on the observation that easy samples can be recognized over relatively smaller inputs while hard samples typically require larger inputs to explore finer details, considerable computations can be reduced by

unevenly distributing computations among samples. Such related implementations include (1) resolution switcher [32, 47, 51], i.e., dynamically switching between different input resolutions to provide confident enough predictions for each sample under limited computational costs; (2) attending to task-relevant regions [10, 41, 46], e.g., only focusing on the small task-relevant regions for recognition while stopping processing other irrelevant spatial regions for computation savings. Despite great progress in 2D image domain, such spatial redundancy has been relatively few visited in video tasks [32, 40], especially in CSLR, while we are interested in whether it can be further combined with temporal redundancy for higher efficiency.

3 METHOD

Inspired by the fact that videos can be perfectly translated into correct sentences with only a small portion of frames in a lot of scenarios, we seek to save the computations spent on redundant frames for efficiency. Furthermore, we notice the expensive computations spent on fixed high-resolution input (e.g., 224×224) may not always be necessary. For example, easy samples can be easily distinguished with small blurry frames (e.g., 96×96) while hard samples may require fine details contained in high-resolution inputs. To achieve efficient inference, we first propose an adaptive framework, coined as AdaBrowse, to only process partial inputs by leveraging the temporal redundancy, where considerable computational costs can be saved without sacrificing accuracy. We further update it by introducing the inherent spatial redundancy in images by considering frame resolution, referred to as AdaBrowse+.

3.1 AdaBrowse

3.1.1 Overview. We first give an overview of AdaBrowse in fig. 2. Given an input sequence, AdaBrowse needs to dynamically select a suitable input sequence length for the attached CSLR model to maximize accuracy under limited computational budgets. For this goal, a Global CNN f_G is first utilized to take a quick glance at the input sequence, obtaining coarse and cheap features. For efficient inference, this procedure is required to be as lightweight as possible. Thus, we let the Global CNN f_G scan input of relatively lower resolutions (e.g., 96×96) which only consumes small extra computations. Then, these features are fed into a policy network π to holistically consider information across frames to select an appropriate input length from M subsequence candidates. Once the decision is made, a corresponding subsequence will be selected and fed into a common Local 2D CNN f_L to extract frame-wise features followed by a recognition model to predict sentences. The features extracted by f_G will be reused and inferred by a lightweight recognition model, whose outputs are averaged with those from another branch as final predictions. We will detail these components in the following.

3.1.2 Global CNN f_G and Local CNN f_L . The Global CNN f_G is utilized to rapidly process input frames for a quick glance to obtain coarse and cheap global features. Compared to the common Local 2D CNN f_L used to extract expensive but powerful features for the following recognition model, f_G has to be circularly executed for each sample and thus is required to consume as few computations as possible. Therefore, we fed frames of relatively small resolutions

(e.g., 96×96) into f_G to make it quite lightweight and fast, which can still provide reliable global features for the subsequent policy network π to make decisions. Instead, we deploy f_L as a powerful backbone with high-resolution inputs to offer discriminative representations for the recognition model.

Specifically, given T input frames $V=\{v_1, \dots, v_T\}$, f_G will take the resized low-resolution frames as inputs and produce coarse features x_t^G as :

$$x_t^G = f_G(\text{Resize}(v_t)), \quad t \in \mathbb{R}^T. \quad (1)$$

Instead, f_L will process a selected target subsequence into discriminative representations as:

$$x_t^L = f_L(\tilde{v}_t), \quad t \in \mathbb{R}^T \quad (2)$$

where \tilde{v} is the selected subsequence by the policy network π introduced next.

3.1.3 Policy network π . The policy network π receives global coarse features x^G from f_G to select a suitable length for each input sequence to process. The policy network should receive both past and future information to help infer the suitable input subsequence for each video. Besides, it's better to browse the input video backward and forward to obtain an overall perspective of the input video. Thus, we instantiate the policy network π as a GRU [4] to aggregate cross-frame information, which is followed by a MLP to predict which subsequence to use. The outputs of the MLP is a vector c with size of \mathbb{R}^{2^M-1} , which predicts the distribution of selecting 2^M-1 subsequences.

For the subsequence generation, we divide the input into subsequences with different lengths beforehand. Formally, with predefined M kinds of subsequence length, we sample inputs with interval $\{1, \dots, 2^{M-1}\}$. The resulted subsequences own $\{1, \dots, \frac{1}{2^{M-1}}\}$ length compared to the inputs. To enrich the action representation diversity, for m_{th} subsequence, we sample it with different starting and ending offsets by $\{1, \dots, 2^{m-1}\}$, resulting in 2^{m-1} subspecies. Thus, there would be totally $\{1+2^1 + \dots, 2^{M-1}\} = 2^M - 1$ subsequence candidates.

Specifically, as π selects a subsequence from $2^M - 1$ candidates, it leads to a non-differentiable problem. We refer to the Gumbel-Softmax Algorithm [24] to solve this discrete sampling issue. In specific, the choice $c \in \mathbb{R}^{2^M-1}$ of the selected subsequence is drawn from the distribution:

$$c \sim \pi(\cdot | x^G, h^\pi) \quad (3)$$

where h^π is the hidden state of the final timestep in GRU. Once the choice c is generated, it will be transposed into a one-hot vector and multiplied with subsequence candidates to select a target one for further processing.

3.1.4 Gumbel-Softmax Algorithm. We refer to the Gumbel-Softmax Algorithm[24] to help resolve the non-differentiable problem in sampling c from a discrete distribution, and make it differentiable to allow backward gradient flow. In specific, given the normalized logits $z \in \mathbb{R}^M$ generated by π for predicting c , the Gumbel-Softmax Algorithm adds Gumbel noise $g \in \mathbb{R}^M$ to z and then draw a discrete sample:

$$\tilde{z} = \underset{i \in M}{\operatorname{argmax}}(z^i + g^i). \quad (4)$$

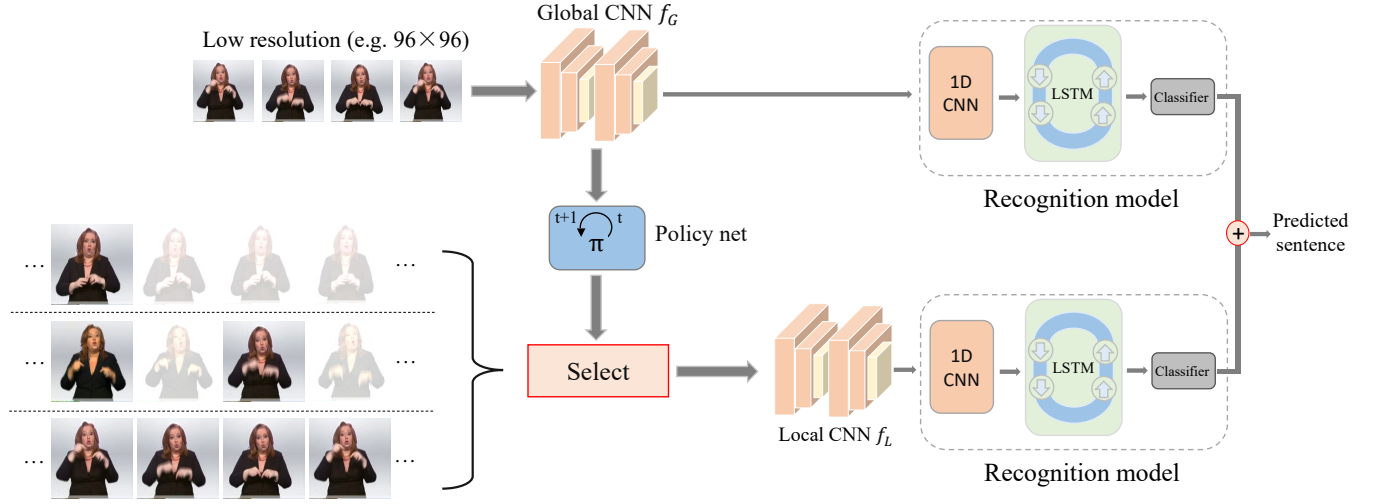


Figure 2: An overview for AdaBrowse. A lightweight Global CNN f_G is first employed to extract coarse features. These features are then sent into a policy network π to select a target subsequence which is finally inferred by an attached recognition model. Features extracted by f_G are reused and inferred by another lightweight recognition model and outputs from two branches are averaged as final predictions.

Here $g^i = -\log(-\log U_i)$ represents a standard Gumbel distribution with U_i sampled from a uniform i.i.d distribution $U(0, 1)$. \tilde{z} is used to choose frame resolution in the network forward pass. Due to the non-differentiable property of argmax operation in Eq. 4, the Gumbel-Softmax distribution is used as a continuous relaxation for argmax to allow back propagating from the discrete sample. In specific, the one-hot coding of \tilde{z} is relaxed to a normalized distribution \hat{z} using softmax:

$$\hat{z}^i = \frac{\exp((\log(z^i) + g^i)/\tau)}{\sum_{i=0}^C \exp((\log(z^i) + g^i)/\tau)} \quad (5)$$

where τ is a temperature parameter that controls the approximation degree of \hat{z} to \tilde{z} . When $\tau \rightarrow +\infty$, \hat{z} becomes uniform distribution. While $\tau \rightarrow 0$, \hat{z} approaches a one-hot vector i.e., \tilde{z} . In practice, τ is always set as a big value and then annealed down to approaching 0 as training progresses.

3.1.5 Recognition model. The recognition model receives preceding representations x_L from f_L and x_G from f_G to produce predicted sentences. We set the recognition model as a series of 1D CNN, a BiLSTM and a fully connected layer, following state-of-the-art CSLR methods [17, 34]. In this sense, our model can be viewed for fair comparison with current CSLR methods, which only equips with additional lightweight f_G , π and another recognition model to adaptively make decisions.

3.2 Training Algorithm

3.2.1 Training procedure. To better cooperate different components in AdaBrowse with each other, we present a two-stage training algorithm.

Stage I: Warm-up. We first equip f_G and f_L with the recognition model e_G and e_L over their corresponding input resolutions to prepare well-initialized parameters separately, by training with the

standard CTC loss [15] over the training set D_{train} :

$$\underset{f_L, e_L, f_G, e_G}{\text{minimize}} \quad \mathbb{E}_{V_i \in D_{train}} \left[\frac{1}{N} \sum_{i=0}^N \mathcal{L}_{CTC}(p_i, y_i) \right] \quad (6)$$

where p_i and y_i denotes the prediction and ground truth label of V_i in D_{train} , respectively, and i is the index number.

Stage II: Cooperation. Given the well-initialized parameters for f_G , f_L , e_G and e_L , we cooperate them within a whole framework. Specifically, a low-resolution input is first fed into f_G to produce coarse features, which will both undergo π to provide decisions c and get through e_G to obtain sentence predictions p^G . Then features of $2^M - 1$ subsequence candidates are multiplied with the transposed one-hot vector of c to produce a selected subsequence, which will be sent into f_L and e_L to produce sentence predictions p^L . Finally, p^G and p^L will be averaged to give final outputs. The training goal can be presented as:

$$\underset{f_L, e_L, f_G, e_G, \pi}{\text{minimize}} \quad \mathbb{E}_{V_i \in D_{train}} \frac{1}{N} \sum_{i=0}^N \left[\mathcal{L}_{CTC}(p_i^G, y_i) + \mathcal{L}_{CTC}(p_i^L, y_i) + \alpha \mathcal{L}_{Effi} + \beta \mathcal{L}_{Align} \right]$$

Here, \mathcal{L}_{Effi} and \mathcal{L}_{Align} denote the efficiency loss and alignment loss, with α and β representing their weights, respectively. We will introduce them next.

3.2.2 Loss functions. Except for the standard CTC Loss [15] to align target sentences with predicted sentences, we propose another two loss functions \mathcal{L}_{Effi} and \mathcal{L}_{Align} to balance between accuracy and computational costs, and coordinate them with the network components in AdaBrowse for additional supervision.

CTC Loss \mathcal{L}_{CTC} . It aligns an input video $\mathcal{V} = (v_1, \dots, v_T)$ with a target sentences with U glosses, $\mathcal{G} = (g_1, \dots, g_U)$. Specifically, CTC loss introduces a blank label (-) to represent unlabeled data

(non-gesture segments or transitional frames) in the target sentence. Then CTC loss builds a many-to-one function \mathcal{B} , to align input frames with output glosses referred to as path l by removing the repeated and blank label in the target sentence, e.g. $\mathcal{B}(\text{-S-u-n-n-d-a-a-y-}) = \mathcal{B}(\text{-S-u-n-d-a-y-}) = \text{Sunday}$. With the help of this mapping function \mathcal{B} , CTC loss provides end-to-end supervision for the parameters of the model by summing the probabilities of all feasible paths:

$$\begin{aligned} \mathcal{L}_{\text{CTC}} &= -\log p(\mathcal{G}|\mathcal{V};\theta) \\ &= -\log\left(\sum_{l \in \mathcal{B}^{-1}(\mathcal{G})} p(l|\mathcal{V};\theta)\right). \end{aligned} \quad (7)$$

Based on the conditional independence assumption, the conditional probability $p(l|\mathcal{V})$ can be calculated as follows:

$$p(l|\mathcal{V};\theta) = \prod_{t=1}^T p(l_t|\mathcal{V};\theta) \quad (8)$$

where the probabilities are exactly the normalized output logits generated by the network classifier.

Efficiency loss \mathcal{L}_{Eff} . Specifically, we precalculate a computation table $s \in \mathbb{R}^{2^M-1}$ in advance to save the computations of processing $2^M - 1$ subsequences. The efficiency loss \mathcal{L}_{Eff} can be computed by multiplying the one-hot vector c with s , to query the computations of as:

$$\mathcal{L}_{\text{Eff}} = c \times s. \quad (9)$$

It can be set as different values to produce a set of models under various demands.

Alignment Loss $\mathcal{L}_{\text{Align}}$. Considering f_L and f_G are pretrained over different resolutions, the representations x_G generated by f_G will mostly be less powerful than x_L generated by f_L . We propose $\mathcal{L}_{\text{Align}}$ to further enhance f_G to provide more stable decisions c and better sentence predictions p^G by distilling valuable features from x_L to x_G with Kullback-Leibler divergence as:

$$\mathcal{L}_{\text{Align}} = \text{KL}\left(\text{softmax}\left(\frac{x^G}{\gamma}\right), \text{softmax}\left(\frac{x^L}{\gamma}\right)\right) \quad (10)$$

where γ controls the "soften" degree and is set as 8.

3.3 Reducing Spatial Redundancy

Except for temporal redundancy, we notice that lots of "easy" videos can be perfectly recognized over smaller inputs (low resolution), where identically feeding the model with high-resolution frames may be unnecessary, and inevitably wastes plenty of computations. We propose an extended version of AdaBrowse, coined as AdaBrowse+, by incorporating frame resolution decision into our framework.

Given partitioned subsequences, we further divide each subsequence into R different resolutions from the lowest to the highest (normal input), to be holistically aware of spatial-temporal redundancy. With R resolution candidates, we always feed the lowest resolution into f_G to extract coarse features x_G with the goal of saving computations. x_G will be sent into π to make decisions over both resolutions and subsequences. As a full sequence of the lowest resolution has been processed, it won't be further divided into shorter subsequences and thus the number of all candidates

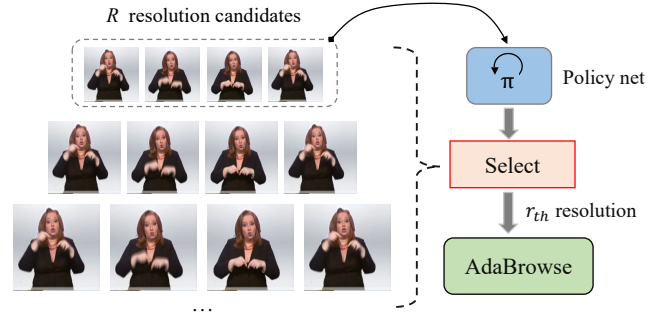


Figure 3: An overview for the updated part in AdaBrowse+.

is $(R - 1) \times (2^M - 1) + 1$. The precalculated computation table s in \mathcal{L}_{Eff} is expanded as well.

4 EXPERIMENTS

4.1 Experimental Setup

Datasets. PHOENIX14 [26] and PHOENIX14-T [1] are both recorded from the German TV weather forecasts. All actions are performed by nine actors wearing dark clothes in front of a clean background. They contain 6841/8247 different sentences with a vocabulary of size 1296/1085 which are split into 5672/7096 training samples, 540/519 development (Dev) samples and 629/642 testing (Test) samples. CSL-Daily [49] revolves the daily life, recorded indoors at 30fps by 10 signers. It contains 20654 sentences, divided into 18401 training samples, 1077 development (Dev) samples and 1176 testing (Test) samples. CSL [22] is recorded in the laboratory by 15 signers with a vocabulary size of 178 with 100 sentences. 25000 videos are divided into training/testing sets by 8:2.

Implementation details. Stage I: The training procedure follows identical settings with recent CSLR methods [3, 34–36] for fair comparison. ResNet18 [18] with ImageNet [8] pretrained weights is adopted for f_L and f_G . The recognition model is consisted of 1D CNNs, a two-layer BiLSTM of hidden size 1024 and a fully connected layer, where sequential layers of {K5, P2, K5, P2} are adopted as 1D CNNs and $K\sigma$ and $P\sigma$ denotes a 1D convolutional layer and a max pooling layer with kernel size σ , respectively. Totally, we train models for 40 epochs with batch size 2 on a 3090 GPU. Adam optimizer is used with weight decay 10^{-4} and an initial learning rate of 10^{-4} , divided by five after 20 and 30 epochs. Input frames are first resized to 256×256 and randomly cropped to 224×224 during training, augmented with 50% random horizontal flip, and $\pm 20\%$ random temporal scaling. During testing, a center 224×224 crop is simply adopted. Following VAC [34], two losses, i.e. VA Loss and VE Loss are added for additional visual supervision. The weight of VA Loss and VE Loss are set as 25.0 and 1.0 respectively. We offer three choices ($M=3$) for subsequences, i.e. $\frac{1}{4}$, $\frac{1}{2}$ and 1, and three resolution candidates ($R=3$), i.e. 224×224 , 160×160 and 96×96 . Thus the number of all candidates is 7.

Stage II: Generally, the training procedure follows similar settings with Stage I, excepting only training for 30 epochs with learning rate of 10^{-4} , divided by five after 10 and 20 epochs, respectively. \mathcal{L}_{Eff} is employed to coordinate the internal components whose

Table 1: Results for AdaBrowse and AdaBrowse+ on the PHOENIX14, PHOENIX14-T, CSL-Daily and CSL datasets. Throughput is measured on a 3090 graphical card with data cached and batch size 1.

Methods	α	GFLOPs	Throughput (videos/s)	PHOENIX14		PHOENIX14-T		CSL-Daily		CSL
				Dev(%)	Test(%)	Dev(%)	Test(%)	Dev(%)	Test(%)	
Baseline	-	364	12.22	19.7	20.9	19.5	20.8	31.5	30.8	0.9
AdaBrowse	0.04	287	12.31	19.4	20.5	19.3	20.5	31.1	30.6	0.6
AdaBrowse	0.15	254	14.26	19.6	20.8	19.4	20.6	31.3	30.6	0.8
AdaBrowse+	0.05	241	15.12	19.4	20.5	19.4	20.5	31.1	30.6	0.6
AdaBrowse+	0.10	171 ($\downarrow 2.12\times$)	17.58 ($\uparrow 1.44\times$)	19.6	20.7	19.5	20.6	31.2	30.7	0.7

Table 2: Comparison of AdaBrowse with lightweight backbones on the PHOENIX14 dataset.

Backbones	Throughput (videos/s)	PHOENIX14	
		Dev(%)	Test(%)
Baseline(ResNet18 [18])	12.22	19.7	20.9
RegNetX-800mf [38]	12.55	19.9	21.1
SqueezeNet [23]	13.13	21.6	22.3
ShuffleNet V2 [31]	12.35	20.7	22.1
MobileNet V2 [19]	12.35	21.3	22.5
EfficientNet B0 [39]	12.35	21.4	22.5
AdaBrowse	14.26	19.6	20.8
AdaBrowse+	17.58	19.6	20.7

weight α is set within [0.04, 0.15] to produce a set of models to balance between accuracy and computations.

Evaluation Metric. We use word error rate (WER) to evaluate the performance of recognition, which is defined as the minimal summation of the **substitution**, **insertion** and **deletion** operations to convert the predicted sentence to the reference sentence as:

$$\text{WER} = \frac{\#\text{sub} + \#\text{ins} + \#\text{del}}{\#\text{reference}}. \quad (11)$$

Note that the **lower** WER, the **better** accuracy.

4.2 Analytical Results

For clarity, we denote λR_η as a subsequence with λ input length over resolution of $\eta \times \eta$. For example, $\frac{1}{4}R_{224}$ denotes a $\frac{1}{4}$ subsequence over resolution of 224×224 . We use R_{224} as our baseline.

Effectiveness. We show the effectiveness of AdaBrowse and AdaBrowse+ on the PHOENIX14, PHOENIX14-T, CSL-Daily and CSL datasets in tab. 1. Notably, our AdaBrowse generalizes well upon different datasets that are shot over various environments and expressed with different sign languages. Our baseline consumes 364G FLOPs of computations and achieves a throughput of 12.22 videos/s. By incorporating temporal feature redundancy into consideration, our proposed AdaBrowse notably decreases the required FLOPs to 254G and raises the throughput to 15.12 videos/s, retaining comparable accuracy. By further incorporating the spatial feature redundancy into the paradigm, our proposed AdaBrowse+ further increases the efficiency by reducing the FLOPs to 171G ($\downarrow 2.12\times$) and promoting the throughput to 17.58 videos/s (1.44 \times). \mathcal{L}_{Eff} controls the computation-WER trade-off. As the weight for \mathcal{L}_{Eff} increases, the WER is observed to degrade slightly with significantly reduced FLOPs and promoted throughput.

Table 3: Comparison of AdaBrowse with other adaptive methods on the PHOENIX14 dataset.

Backbones	GFLOPs	Throughput (videos/s)	PHOENIX14	
			Dev(%)	Test(%)
Baseline	364	12.22	19.7	20.9
AdaFocus [40]	232	13.62	21.0	22.1
Ar-net [32]	254	13.87	20.2	21.2
AdaFrame [45]	217	14.12	23.6	24.3
AdaBrowse	254	14.26	19.6	20.8
AdaBrowse+	171	17.58	19.6	20.7

Comparison with lightweight backbones. Various lightweight CNNs have been proposed recently for efficiency. We compare AdaBrowse with some widely-used lightweight backbones by replacing f_l with them in tab. 2. It’s observed that although these backbones could slightly promote the throughput, they mostly lead to a drastic accuracy drop. Our AdaBrowse and AdaBrowse+ not only achieve much better throughput but also outperform them on accuracy.

Comparison with other adaptive methods. As no adaptive methods for CSLR have been explored before, we manually reproduce some approaches for CSLR to show the effectiveness of AdaBrowse. AdaFocus [40] dynamically attends to the most informative small region in each frame to save unnecessary computations. Ar-net [32] adaptively decides the frame resolution for each frame to avoid evenly allocating computing resources among frames. AdaFrame [45] tries to only sample a portion of input frames for recognition and discard the rest. Notably, these methods mostly solely consider the temporal redundancy or the spatial redundancy. As shown in tab. 3, these methods always lead to degraded accuracy. Our AdaBrowse series achieve much better accuracy than them with much higher throughput and fewer computations.

Behavior analysis. We are interested in how AdaBrowse internally makes decisions to balance between accuracy and computations. We plot the visualizations of the selected ratio v.s. FLOPs for each candidate in Adabrowse+ in fig. 4. Candidates in the horizontal axis are arranged in reverse order (small \rightarrow big) by their FLOPs over each video. It’s observed that AdaBrowse+ tends to mainly (66%) select $\frac{1}{2}R_{160}$ and almost evenly choose the rest. By incorporating spatial-temporal redundancy into consideration, AdaBrowse+ could dynamically choose to use a lower resolution (160×160) than normal design with partial inputs ($\frac{1}{2}$), satisfying the need for accurate recognition.

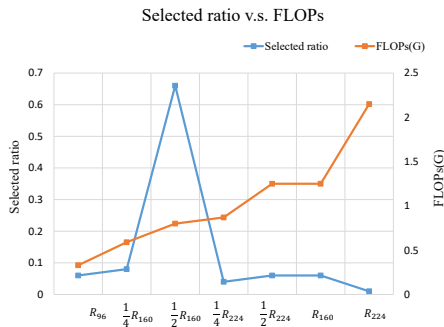


Figure 4: Selected ratio v.s. FLOPs for seven candidates of AdaBrowse+.

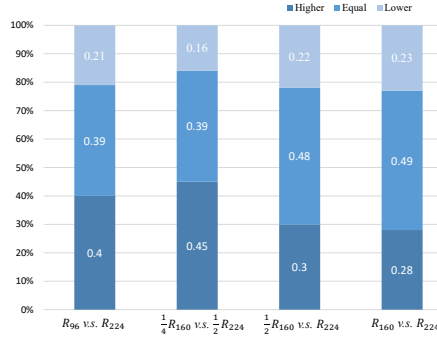


Figure 5: WER comparison over all input videos for some candidates against R_{224} .

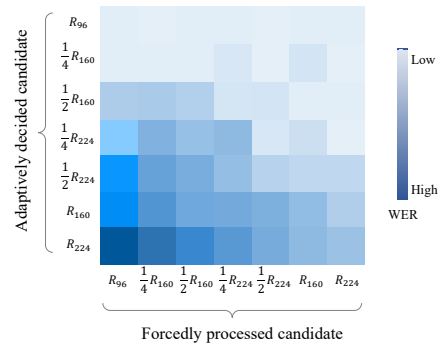


Figure 6: Illustration of WER with respect to processing order of candidates.

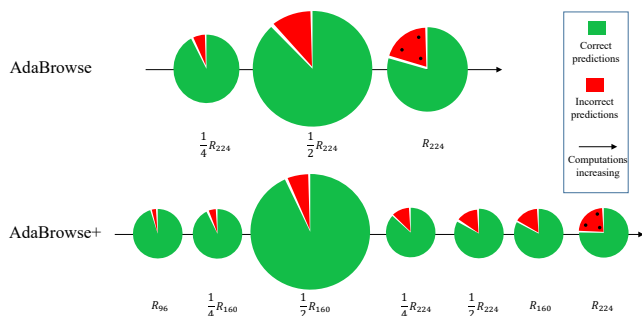


Figure 7: Watermelon visualization for AdaBrowse and AdaBrowse+ over candidates. The area of a circle represents the percentage of processed videos for each candidate. Easier videos are processed by lightweight candidates with higher accuracy while only hard videos reach heavy candidates leading to increased misclassifications.

We further explore why AdaBrowse+ tends to make above decisions. We compare the WER between some candidates (R_{96} , $\frac{1}{4}R_{160}$ and $\frac{1}{2}R_{160}$) and the most expensive R_{224} (which should give most accurate predictions) in fig. 5. It’s noticed that in $>60\%$ input samples, all these candidates can give equal or better predictions compared to R_{224} with much fewer computations. $\frac{1}{2}R_{160}$ achieves the most superior trade-off. It gains competing accuracy compared to R_{160} but consumes much fewer computations. This may result in its wide usage in decisions of AdaBrowse+. An extra detail is the chance of gaining equal or better predictions by $\frac{1}{2}R_{160}$ (70%) compared to R_{224} is quite close to its chance (66%) selected by AdaBrowse+, demonstrating the intelligence over making decisions.

We further analyze the effectiveness of AdaBrowse in fig. 7 by illustrating the prediction accuracy v.s. the number of processed videos for each candidate in AdaBrowse and AdaBrowse+. A possibly counterintuitive observation is that as videos proceed to heavier candidates, the predictions become more inaccurate. However, the reason behind this is that easy videos have exited from earlier lightweight candidates, while only hard videos are left for heavy ones, thus leaving poorer accuracy. This phenomenon can be further

verified in fig. 6 where the vertical axis denotes the candidate adaptively decided by AdaBrowse+ and the horizontal axis denotes the forcedly processed candidate for a video. Interestingly, we notice that if a video is processed by heavier candidates with more computations, no significant accuracy is gained. In contrast, if it’s dealt with more lightweight candidates, a considerable accuracy drop is witnessed, which reflects the intelligence of AdaBrowse to allocate computing resources.

Comparison with the state-of-the-art. Tab. 6, tab. 7 and tab. 8 compare our model with state-of-the-art methods [3, 7, 29, 34, 35, 35–37, 50] over both WER and FLOPs. AdaBrowse and AdaBrowse+ not only achieve state-of-the-art accuracy, but also significantly lower the required GFLOPs, which achieves the best WER-computation trade-off. Notably, AdaBrowse series reduce required computations to only half compared to existing methods. Hopefully, AdaBrowse makes a step further towards real-life deployment of sign language understanding.

4.3 Ablation Study

Effectiveness of adaptive policy is verified in tab. 7 against random sampling and sampling from a Gaussian distribution. It’s observed our adaptive policy outperforms these counterparts by a large margin over accuracy, demonstrating its effectiveness.

Effects of reusing x_G for recognition is ablated in tab. 8, where only using x_L for recognition degrades the accuracy by about 0.4%–0.5%. Two-branch fusion could take advantage of features from different hierarchies.

Effects of \mathcal{L}_{Align} is verified in tab. 9. $\beta = 0$ means \mathcal{L}_{Align} is disabled. It’s observed that as β increases, AdaBrowse achieves better accuracy as well. Thus \mathcal{L}_{Align} could help f_G to obtain more representative features by mimicking f_L . β is set as 25.0 by default.

4.4 Online Setting

Consider the online scenario in the real-world scenarios, where a stream of frames comes in sequentially and the model may need to output the sentence prediction at any time. We test our AdaBrowse in this case to show its effectiveness in the real-world applications. Specifically, we follow FCN [3] to build a fully convolutional network as a baseline, which only watches information from the current and past timesteps to make sentence predictions, and deploy

Table 4: Comparison with other methods over both WER and FLOPs on the PHOENIX14 and PHOENIX14-T datasets. ★ means additional factors such as face and hands are used. AdaBrowse and AdaBrowse+ achieve the best WER-computation trade-off.

Methods	Backbone	GFLOPs per video	PHOENIX14				PHOENIX14-T	
			Dev(%)		Test(%)		Dev(%)	Test(%)
			del/ins	WER	del/ins	WER		
FCN [3]	Custom	286	-	23.7	-	23.9	23.3	25.1
CMA [36]	GoogLeNet	316	7.3/2.7	21.3	7.3/2.4	21.9	-	-
VAC [34]	ResNet18	367	7.9/2.5	21.2	8.4/2.6	22.3	-	-
SMKD [17]	ResNet18	367	6.8/2.5	20.8	6.3/2.3	21.0	20.8	22.4
TLP [20]	ResNet18	367	6.3/2.8	19.7	6.1/2.9	20.8	19.4	21.2
SEN [21]	ResNet18	367	5.8/2.6	19.5	7.3/4.0	21.0	19.3	20.7
SLT* [1]	GoogLeNet	316	-	-	-	-	24.5	24.6
CNN+HMM+LSTM* [25]	GoogLeNet	316	-	26.0	-	26.0	22.1	24.1
STMC* [50]	VGG11	1554	7.7/3.4	21.1	7.4/2.6	20.7	19.6	21.0
C ² SLR* [52]	ResNet18	367	-	20.5	-	20.4	20.2	20.4
AdaBrowse	ResNet18	254	6.0/2.6	19.6	6.0/2.8	20.8	19.4	20.6
AdaBrowse+	ResNet18	171	6.0/2.5	19.6	5.9/2.6	20.7	19.5	20.6

Table 5: Comparison with state-of-the-art methods on the CSL-Daily dataset [49].

Methods	GFLOPs per video	Dev(%)	Test(%)
LS-HAN [22]	-	39.0	39.4
TIN-Iterative [49]	632	32.8	32.4
Joint-SLRT [2]	316	33.1	32.0
FCN [3]	286	33.2	32.5
BN-TIN [49]	316	33.6	33.1
AdaBrowse	254	31.3	30.6
AdaBrowse+	171	31.2	30.7

Table 6: Comparison with state-of-the-art methods on the CSL dataset [22].

Methods	GFLOPs per video	WER(%)
SubUNet [5]	-	11.0
SF-Net [48]	364	3.8
FCN [3]	286	3.0
STMC [50]	1554	2.1
VAC [34]	364	1.6
AdaBrowse	254	0.8
AdaBrowse+	171	0.7

Table 7: Effects of adaptive policy of AdaBrowse+.

Methods	PHOENIX14		PHOENIX14-T	
	Dev(%)	Test(%)	Dev(%)	Test(%)
Adaptive	19.6	20.7	19.5	20.6
Random	20.7	22.9	20.9	23.1
Gaussian	20.6	23.1	21.1	23.0

our AdaBrowse upon it. We use video frames from the PHOENIX14 dataset to mimic the shot videos in the real life. Tab. 10 shows the

Table 8: Effects of reusing x_G for recognition.

Reusing x_G	PHOENIX14		PHOENIX14-T	
	Dev(%)	Test(%)	Dev(%)	Test(%)
✗	20.1	21.2	20.0	21.2
✓	19.6	20.7	19.5	20.6

Table 9: Effects of \mathcal{L}_{Align} for recognition.

β	0.0	10.0	20.0	25.0	30.0	50.0
Dev(%)	20.1	19.9	19.7	19.6	19.8	20.0
Test(%)	21.2	21.1	20.9	20.7	20.8	21.0

Table 10: Effectiveness of AdaBrowse in the online setting.

Methods	Throughput	GFLOPs	WER
Baseline	11.24	361	21.0
AdaBrowse	15.84 ($\uparrow 1.41\times$)	175 ($2.06\downarrow$)	20.8

results. It's observed that compared to the baseline, our AdaBrowse could effectively promote the number of processed videos to 1.41× with 2.06 fewer FLOPs. Meanwhile, our AdaBrowse could achieve slightly better accuracy than the baseline. These results verify the effectiveness of our AdaBrowse in applications of real-world scenario, which may bridge the communication gap of hearing-impaired people and the hearing people.

5 CONCLUSION

We propose AdaBrowse towards efficient CSLR by dynamically selecting a most informative subsequence over multiple resolutions. Considerable efficiency is achieved by considering the temporal redundancy and is further promoted by incorporating spatial redundancy, with 1.44× throughput over 2.12× less FLOPs.

ACKNOWLEDGMENTS

This work is supported by the National Natural Science Foundation of China (Project No. 62072334).

REFERENCES

- [1] Necati Cihan Camgoz, Simon Hadfield, Oscar Koller, Hermann Ney, and Richard Bowden. 2018. Neural sign language translation. In *Proceedings of the IEEE Conference on Computer Vision and Pattern Recognition*. 7784–7793.
- [2] Necati Cihan Camgoz, Oscar Koller, Simon Hadfield, and Richard Bowden. 2020. Sign language transformers: Joint end-to-end sign language recognition and translation. In *Proceedings of the IEEE/CVF conference on computer vision and pattern recognition*. 10023–10033.
- [3] Ka Leong Cheng, Zhaoyang Yang, Qifeng Chen, and Yu-Wing Tai. 2020. Fully convolutional networks for continuous sign language recognition. In *European Conference on Computer Vision*. Springer, 697–714.
- [4] Kyunghyun Cho, Bart Van Merriënboer, Caglar Gulcehre, Dzmitry Bahdanau, Fethi Bougares, Holger Schwenk, and Yoshua Bengio. 2014. Learning phrase representations using RNN encoder-decoder for statistical machine translation. *arXiv preprint arXiv:1406.1078* (2014).
- [5] Necati Cihan Camgoz, Simon Hadfield, Oscar Koller, and Richard Bowden. 2017. Subnets: End-to-end hand shape and continuous sign language recognition. In *Proceedings of the IEEE International Conference on Computer Vision*. 3056–3065.
- [6] Rungpeng Cui, Hu Liu, and Changshui Zhang. 2017. Recurrent convolutional neural networks for continuous sign language recognition by staged optimization. In *Proceedings of the IEEE conference on computer vision and pattern recognition*. 7361–7369.
- [7] Rungpeng Cui, Hu Liu, and Changshui Zhang. 2019. A deep neural framework for continuous sign language recognition by iterative training. *IEEE Transactions on Multimedia* 21, 7 (2019), 1880–1891.
- [8] Jia Deng, Wei Dong, Richard Socher, Li-Jia Li, Kai Li, and Li Fei-Fei. 2009. Imagenet: A large-scale hierarchical image database. In *2009 IEEE conference on computer vision and pattern recognition*. Ieee, 248–255.
- [9] Hehe Fan, Zhongwen Xu, Linchao Zhu, Chenggang Yan, Jianjun Ge, and Yi Yang. 2018. Watching a small portion could be as good as watching all: Towards efficient video classification. In *IJCAI International Joint Conference on Artificial Intelligence*.
- [10] Michael Figurnov, Maxwell D Collins, Yukun Zhu, Li Zhang, Jonathan Huang, Dmitry Vetrov, and Ruslan Salakhutdinov. 2017. Spatially adaptive computation time for residual networks. In *Proceedings of the IEEE Conference on Computer Vision and Pattern Recognition*. 1039–1048.
- [11] William T Freeman and Michal Roth. 1995. Orientation histograms for hand gesture recognition. In *International workshop on automatic face and gesture recognition*, Vol. 12. IEEE Computer Society, Washington, DC, 296–301.
- [12] Ruohan Gao, Tae-Hyun Oh, Kristen Grauman, and Lorenzo Torresani. 2020. Listen to look: Action recognition by previewing audio. In *Proceedings of the IEEE/CVF Conference on Computer Vision and Pattern Recognition*. 10457–10467.
- [13] Wen Gao, Gaolin Fang, Debin Zhao, and Yiqiang Chen. 2004. A Chinese sign language recognition system based on SOFM/SRN/HMM. *Pattern Recognition* 37, 12 (2004), 2389–2402.
- [14] Amir Ghodrati, Babak Ehteshami Bejnordi, and Amirhossein Habibian. 2021. Frameexit: Conditional early exiting for efficient video recognition. In *Proceedings of the IEEE/CVF Conference on Computer Vision and Pattern Recognition*. 15608–15618.
- [15] Alex Graves, Santiago Fernández, Faustino Gomez, and Jürgen Schmidhuber. 2006. Connectionist temporal classification: labelling unsegmented sequence data with recurrent neural networks. In *Proceedings of the 23rd international conference on Machine learning*. 369–376.
- [16] Junwei Han, George Awad, and Alistair Sutherland. 2009. Modelling and segmenting subunits for sign language recognition based on hand motion analysis. *Pattern Recognition Letters* 30, 6 (2009), 623–633.
- [17] Aiming Hao, Yuecong Min, and Xilin Chen. 2021. Self-Mutual Distillation Learning for Continuous Sign Language Recognition. In *Proceedings of the IEEE/CVF International Conference on Computer Vision*. 11303–11312.
- [18] Kaiming He, Xiangyu Zhang, Shaoqing Ren, and Jian Sun. 2016. Deep residual learning for image recognition. In *Proceedings of the IEEE conference on computer vision and pattern recognition*. 770–778.
- [19] Andrew Howard, Andrey Zhmoginov, Liang-Chieh Chen, Mark Sandler, and Menglong Zhu. 2018. Inverted residuals and linear bottlenecks: Mobile networks for classification, detection and segmentation. (2018).
- [20] Lianyu Hu, Liqing Gao, Zekang Liu, and Wei Feng. 2022. Temporal lift pooling for continuous sign language recognition. In *Computer Vision—ECCV 2022: 17th European Conference, Tel Aviv, Israel, October 23–27, 2022, Proceedings, Part XXXV*. 511–527.
- [21] Lianyu Hu, Liqing Gao, Zekang Liu, and Wei Feng. 2023. Self-Emphasizing Network for Continuous Sign Language Recognition. In *Thirty-seventh AAAI conference on artificial intelligence*.
- [22] Jie Huang, Wengang Zhou, Qilin Zhang, Houqiang Li, and Weiping Li. 2018. Video-based sign language recognition without temporal segmentation. In *Proceedings of the AAAI Conference on Artificial Intelligence*, Vol. 32.
- [23] Forrest N Iandola, Song Han, Matthew W Moskewicz, Khalid Ashraf, William J Dally, and Kurt Keutzer. 2016. SqueezeNet: AlexNet-level accuracy with 50x fewer parameters and < 0.5 MB model size. *arXiv preprint arXiv:1602.07360* (2016).
- [24] Eric Jang, Shixiang Gu, and Ben Poole. 2016. Categorical reparameterization with gumbel-softmax. *arXiv preprint arXiv:1611.01144* (2016).
- [25] Oscar Koller, Necati Cihan Camgoz, Hermann Ney, and Richard Bowden. 2019. Weakly supervised learning with multi-stream CNN-LSTM-HMMs to discover sequential parallelism in sign language videos. *IEEE transactions on pattern analysis and machine intelligence* 42, 9 (2019), 2306–2320.
- [26] Oscar Koller, Jens Forster, and Hermann Ney. 2015. Continuous sign language recognition: Towards large vocabulary statistical recognition systems handling multiple signers. *Computer Vision and Image Understanding* 141 (2015), 108–125.
- [27] Oscar Koller, Hermann Ney, and Richard Bowden. 2016. Deep hand: How to train a cnn on 1 million hand images when your data is continuous and weakly labelled. In *Proceedings of the IEEE conference on computer vision and pattern recognition*. 3793–3802.
- [28] Oscar Koller, O Zargaran, Hermann Ney, and Richard Bowden. 2016. Deep sign: Hybrid CNN-HMM for continuous sign language recognition. In *Proceedings of the British Machine Vision Conference* 2016.
- [29] Oscar Koller, Sepehr Zargaran, and Hermann Ney. 2017. Re-sign: Re-aligned end-to-end sequence modelling with deep recurrent CNN-HMMs. In *Proceedings of the IEEE conference on computer vision and pattern recognition*. 4297–4305.
- [30] Bruno Korbar, Du Tran, and Lorenzo Torresani. 2019. Scsampl: Sampling salient clips from video for efficient action recognition. In *Proceedings of the IEEE/CVF International Conference on Computer Vision*. 6232–6242.
- [31] Ningning Ma, Xiangyu Zhang, Hai-Tao Zheng, and Jian Sun. 2018. Shufflenet v2: Practical guidelines for efficient cnn architecture design. In *Proceedings of the European conference on computer vision (ECCV)*. 116–131.
- [32] Yue Meng, Chung-Ching Lin, Rameswar Panda, Prasanna Sattigeri, Leonid Karlinsky, Aude Oliva, Kate Saenko, and Rogerio Feris. 2020. Ar-net: Adaptive frame resolution for efficient action recognition. In *European Conference on Computer Vision*. Springer, 86–104.
- [33] Yue Meng, Rameswar Panda, Chung-Ching Lin, Prasanna Sattigeri, Leonid Karlinsky, Kate Saenko, Aude Oliva, and Rogerio Feris. 2021. Adafuse: Adaptive temporal fusion network for efficient action recognition. *arXiv preprint arXiv:2102.05775* (2021).
- [34] Yuecong Min, Aiming Hao, Xiujuan Chai, and Xilin Chen. 2021. Visual Alignment Constraint for Continuous Sign Language Recognition. In *Proceedings of the IEEE/CVF International Conference on Computer Vision (ICCV)*. 11542–11551.
- [35] Zhe Niu and Brian Mak. 2020. Stochastic fine-grained labeling of multi-state sign glosses for continuous sign language recognition. In *European Conference on Computer Vision*. Springer, 172–186.
- [36] Junfu Pu, Wengang Zhou, Hezhen Hu, and Houqiang Li. 2020. Boosting continuous sign language recognition via cross modality augmentation. In *Proceedings of the 28th ACM International Conference on Multimedia*. 1497–1505.
- [37] Junfu Pu, Wengang Zhou, and Houqiang Li. 2019. Iterative alignment network for continuous sign language recognition. In *Proceedings of the IEEE/CVF Conference on Computer Vision and Pattern Recognition*. 4165–4174.
- [38] Ilija Radosavovic, Raj Prateek Kosaraju, Ross Girshick, Kaiming He, and Piotr Dollár. 2020. Designing network design spaces. In *Proceedings of the IEEE/CVF Conference on Computer Vision and Pattern Recognition*. 10428–10436.
- [39] Mingxing Tan and Quoc Le. 2019. Efficientnet: Rethinking model scaling for convolutional neural networks. In *International conference on machine learning*. PMLR, 6105–6114.
- [40] Yulin Wang, Zhaoxi Chen, Haojun Jiang, Shiji Song, Yizeng Han, and Gao Huang. 2021. Adaptive focus for efficient video recognition. In *Proceedings of the IEEE/CVF International Conference on Computer Vision*. 16249–16258.
- [41] Yulin Wang, Kangchen Lv, Rui Huang, Shiji Song, Le Yang, and Gao Huang. 2020. Glance and focus: a dynamic approach to reducing spatial redundancy in image classification. *arXiv preprint arXiv:2010.05300* (2020).
- [42] Wenhao Wu, Dongliang He, Xiao Tan, Shifeng Chen, and Shilei Wen. 2019. Multi-agent reinforcement learning based frame sampling for effective untrimmed video recognition. In *Proceedings of the IEEE/CVF International Conference on Computer Vision*. 6222–6231.
- [43] Zuxuan Wu, Hengduo Li, Caiming Xiong, Yu-Gang Jiang, and Larry Steven Davis. 2020. A dynamic frame selection framework for fast video recognition. *IEEE Transactions on Pattern Analysis and Machine Intelligence* (2020).
- [44] Zuxuan Wu, Caiming Xiong, Yu-Gang Jiang, and Larry S Davis. 2019. Liteeval: A coarse-to-fine framework for resource efficient video recognition. *Advances in neural information processing systems* 32 (2019).
- [45] Zuxuan Wu, Caiming Xiong, Chih-Yao Ma, Richard Socher, and Larry S Davis. 2019. Adaframe: Adaptive frame selection for fast video recognition. In *Proceedings of the IEEE/CVF Conference on Computer Vision and Pattern Recognition*. 1278–1287.
- [46] Zhenda Xie, Zheng Zhang, Xizhou Zhu, Gao Huang, and Stephen Lin. 2020. Spatially adaptive inference with stochastic feature sampling and interpolation. In *European Conference on Computer Vision*. Springer, 531–548.
- [47] Le Yang, Yizeng Han, Xi Chen, Shiji Song, Jifeng Dai, and Gao Huang. 2020. Resolution adaptive networks for efficient inference. In *Proceedings of the IEEE/CVF Conference on Computer Vision and Pattern Recognition*. 2369–2378.

- [48] Zhaoyang Yang, Zhenmei Shi, Xiaoyong Shen, and Yu-Wing Tai. 2019. SF-Net: Structured feature network for continuous sign language recognition. *arXiv preprint arXiv:1908.01341* (2019).
- [49] Hao Zhou, Wengang Zhou, Weizhen Qi, Junfu Pu, and Houqiang Li. 2021. Improving sign language translation with monolingual data by sign back-translation. In *Proceedings of the IEEE/CVF Conference on Computer Vision and Pattern Recognition*. 1316–1325.
- [50] Hao Zhou, Wengang Zhou, Yun Zhou, and Houqiang Li. 2020. Spatial-temporal multi-cue network for continuous sign language recognition. In *Proceedings of the AAAI Conference on Artificial Intelligence*, Vol. 34. 13009–13016.
- [51] Mingjian Zhu, Kai Han, Enhua Wu, Qiulin Zhang, Ying Nie, Zhenzhong Lan, and Yunhe Wang. 2021. Dynamic Resolution Network. In *Advances in Neural Information Processing Systems 34: Annual Conference on Neural Information Processing Systems 2021, NeurIPS 2021, December 6–14, 2021, virtual*, Marc Aurelio Ranzato, Alina Beygelzimer, Yann N. Dauphin, Percy Liang, and Jennifer Wortman Vaughan (Eds.). 27319–27330. <https://proceedings.neurips.cc/paper/2021/hash/e56954b4f6347e897f954495eab16a88-Abstract.html>
- [52] Ronglai Zuo and Brian Mak. 2022. C2SLR: Consistency-Enhanced Continuous Sign Language Recognition. In *Proceedings of the IEEE/CVF Conference on Computer Vision and Pattern Recognition*. 5131–5140.